Received: 19 May 2023 | Revised: 18 June 2023 | Accepted: 3 August 2023

DOI: 10.1111/iep.12491

INTERNATIONAL JOURNAL OF Experimental Pathology WILEY

ORIGINAL ARTICLE

Panx1 knockout promotes preneoplastic aberrant crypt foci development in a chemically induced model of mouse colon carcinogenesis

Sara Gomes Espírito Santo[1] | **Tereza Cristina Da Silva**[2] | **Bruno Cogliati**[2] | **Luís Fernando Barbisan**[1,3] | **Guilherme Ribeiro Romualdo**[1,3]

[1]Botucatu Medical School, Experimental Research Unit (UNIPEX), Multimodel Drug Screening Platform – Laboratory of Chemically Induced and Experimental Carcinogenesis (MDSP-LCQE), São Paulo State University (UNESP), Botucatu, São Paulo State, Brazil

[2]School of Veterinary Medicine and Animal Science, Department of Pathology, University of São Paulo (USP), São Paulo, São Paulo State, Brazil

[3]Biosciences Institute, Department of Structural and Functional Biology, São Paulo State University (UNESP), São Paulo State, Brazil

Correspondence
Guilherme Ribeiro Romualdo, Botucatu Medical School, Experimental Research Unit (UNIPEX), Multimodel Drug Screening Platform – Laboratory of Chemically Induced and Experimental Carcinogenesis (MDSP-LCQE), São Paulo State University (UNESP), Av. Prof. Mário Rubens Guimarães Montenegro, Botucatu/SP, Brazil.
Email: guilherme.romualdo@unesp.br

Funding information
Coordenação de Aperfeiçoamento de Pessoal de Nível Superior; Fundação de Amparo à Pesquisa do Estado de São Paulo

Abstract

Colorectal cancer, which is the third leading cause of cancer-related deaths worldwide, is a multistep disease, featuring preneoplastic aberrant crypt foci (ACF) as the early morphological manifestation. The roles of hemichannel-forming transmembrane Pannexin 1 (Panx1) protein have not been investigated in the context of colon carcinogenesis yet, although it has contrasting roles in other cancer types. Thus, this study was conducted to examine the effects of Panx1 knockout ($Panx1^{-/-}$) on the early events of chemically induced colon carcinogenesis in mouse. Wild type (WT) and $Panx1^{-/-}$ female C57BL6J mice were submitted to a chemically induced model of colon carcinogenesis by receiving six intraperitoneal administrations of 1,2-dimethylhydrazine (DMH) carcinogen. Animals were euthanized 8 h (week 7) or 30 weeks (week 37) after the last DMH administration in order to evaluate sub-acute colon toxicity outcomes or the burden of ACF, respectively. At week 7, Panx1 genetic ablation increased DMH-induced genotoxicity in peripheral blood cells, malondialdehyde levels in the colon, and apoptosis (cleaved caspase-3) in colonic crypts. Of note, at week 37, $Panx1^{-/-}$ animals showed an increase in aberrant crypts (AC), ACF mean number, and ACF multiplicity (AC per ACF) by 56%, 57% and 20%, respectively. In essence, our findings indicate that Panx1 genetic ablation promotes preneoplastic ACF development during chemically induced mouse colon carcinogenesis, and a protective role of Panx1 is postulated.

KEYWORDS

aberrant crypt foci, C57BL/6J mouse, colon carcinogenesis, dimethylhydrazine

1 | INTRODUCTION

Colorectal cancer (CC) is the third leading cause of cancer-related deaths worldwide, affecting both men and women.[1] (Sung et al., 2021). This disease, which is predominantly sporadic (up to 70% of cases), is closely related to smoking, alcohol intake, obesity, sedentary lifestyle, and a diet rich in processed foods, red meat, and sugary drinks.[2–4] Although new treatments have improved CC-related outcomes mainly in countries with high human development index (HDI), the 5-year relative survival remains at 64.7%, and it is up to 10% for patients with metastatic disease.[3,5] CC develops under the emergence and accumulation of a series of morphological, genetic or epigenetic changes in the epithelial cells. During this multistep process, the aberrant crypt foci (ACF) are the earliest histologic alterations to arise. Morphologically, these lesions organize into clusters of differentially stained crypts with an abnormally thick epithelial lining, and oval to slit-shaped crypt openings. A percentage of these lesions also gather key molecular alterations, such as KRAS mutations and β-catenin mutation/accumulation.[6,7] Both clinical and preclinical assays have documented an association between the presence of ACF and risk for CC development. For these reasons, ACF are considered putative preneoplastic lesions in the human colonic mucosa, although their progression towards CC may depend on multiple features.[6,7] In short-to-medium term chemically induced colon carcinogenesis bioassays in rodents, ACF have already proved their predictive value for the prevention, treatment or progression to CC.[8–11] Although some ACF may gather molecular features that support them as CC precursors, the landscape of molecular alterations within these lesions is still not fully unveiled and the search for molecular targets is warranted.

In this background, the roles of Pannexin 1 (Panx1) protein, and Panx1 hemichannels, have not yet been investigated. The family of three paralog transmembrane proteins called Pannexins (Panx1, Panx2, and Panx3), constitute channels that connect the intra and extracellular environments, enabling the bidirectional exchange of essential small molecules (e.g., ions and ATP).[12,13] Panx1 is the most commonly expressed protein of this family, although Panx family tissue distribution ranges from ubiquitous to very restricted, being paralog-dependent, cell type-specific, and developmentally regulated. Panx1 has been implicated in a myriad of physiological and pathophysiological processes.[12–14] There is little evidence for Panx1 distribution in the normal colon. Diezmos et al.[15] showed that Panx1 is broadly immuno-expressed in all layers of this organ, including the cytoplasm and cell membranes of the enterocytes and goblet cells of the colonic mucosa. In contrast, Panx1 channels are proposed to have critical roles in colonic inflammation, as ATP released from these channels may activate purinergic P2X7 receptors (P2X7R), promoting inflammation by paracrine signalling. Indeed, the chemical blockade of Panx1 channels hindered cytokine-induced inflammation in CC Caco-2 cells and in normal cultured human colon strips.[15] In relation to carcinogenesis, Panx1 overexpression in breast and gastric tumour cells was positively associated with epithelial–mesenchymal transition phenotype-related outcomes, which were reversed by genetic knockdown.[16,17] In cohorts of breast, gastric, and liver cancers, Panx1 overexpression was also positively correlated with poor prognosis and/or tumour inflammation.[17–19] In contrast to these tumour-promoting outcomes, Panx1 was demonstrated to interact with liver Xβ (LXβ) receptors, leading to an increased ATP release and subsequent P2X7R activation, which induced pyropoptosis in human and rodent CC cell lines, acting as a tumour suppressor protein.[20] This Panx1-dependent mechanism was also confirmed in a CT26 xenograft mouse model.[20] In the light of the available findings, the roles of Panx1 in the early stages of colon carcinogenesis are still unknown. Thus, the present study was conducted to examine the effects of Panx1 knockout ($Panx1^{-/-}$) on the early events of chemically induced colon carcinogenesis in mouse. In contrast to other gastrointestinal cancers, our preclinical findings indicate that Panx1 deletion promotes preneoplastic ACF development, and a protective property of this protein in early colon carcinogenesis should be investigated further.

2 | METHODS

2.1 | Experimental design

The global $Panx1^{-/-}$ mouse strain (CMV-Cre/Panx1) in C57BL/6J background was generated as previously described.[21] All animals were obtained from the School of Veterinary Medicine and Animal Science of the University of São Paulo (USP), and kept in Botucatu Medical School of the São Paulo State (UNESP). After a 2-week acclimatisation period, 6-week-old female wild type (WT) and female $Panx1^{-/-}$ C57BL/6J mice ($n = 18$ animals/genotype) received six intraperitoneal (i.p.) administrations of 1,2-dimethylhydrazine colon carcinogen (DMH, 20 mg/kg body weight),[22,23] divided in two cycles of three administrations with a rest week between them, or saline 0.9% vehicle, as shown in Figure 1. At week 7, in order to evaluate the sub-acute toxicity outcomes caused by DMH, animals (6 mice/group/genotype) were euthanized 8 h after the last administration, as this timepoint encompasses the peak of DMH-induced apoptosis.[24] At week 37, the remaining animals (12 mice/group/genotype) were

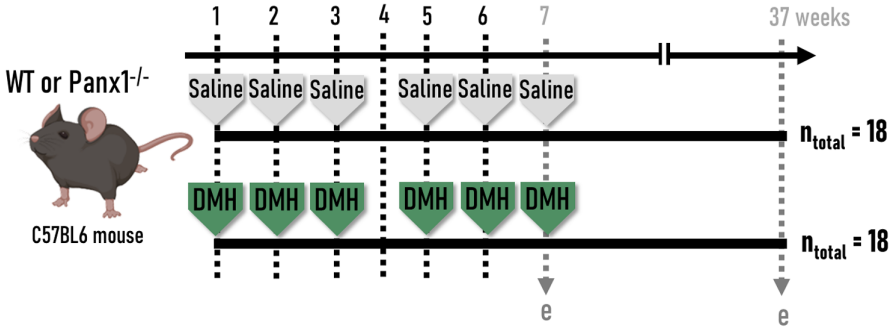

FIGURE 1 Experimental design. Saline: 1 × NaCl 0.9% i.p. administration; DMH: 1 × 20 mg/kg/b.wt. i.p. administration; e: euthanasia; n_{total}: total number of mice per genotype.

euthanized 30 weeks after the last administration, allowing for screening of the earliest microscopic lesions induced by DMH, the preneoplastic ACF.[25] The euthanasia procedures were performed by exsanguination under ketamine/xylazine anaesthesia (100/16 mg/kg body weight, i.p.). The animals received diet and water ad libitum and were kept in polypropylene cages (up to 4 animals/cage) in a room maintained at 22 ± 2°C, 55 ± 10% humidity, and with a 12-h light/dark cycle (light between 07:00 a.m. and 07:00 p.m.). All procedures described herein were approved by the Ethics Committee on Animal Use of the São Paulo State University (UNESP) (#569210721).

At the necropsy, the large intestine was removed, opened longitudinally, and gently rinsed with 0.9% saline to remove residual bowel contents, and the colon length was then measured (cm). At week 7, distal colon samples (1–2 cm) were collected, snap-frozen in liquid nitrogen, and stored at −80°C for biochemical analysis. Other distal colon specimens were fixed in methacarn solution (60% methanol, 30% chloroform, and 10% acetic acid) for 12 h (4°C), transferred to 70% alcohol, and embedded in paraffin. At week 37, the colon was removed and the whole sample was fixed flat in 10% formalin solution for 24 h and transferred to 70% alcohol for ACF analysis. Distal colon was sampled as they display a higher DMH-induced DNA adduct and higher incidence of (pre)neoplastic alterations than middle/proximal colon.[23]

2.2 | Comet assay

Peripheral blood samples from the retro-orbital plexus were obtained 4 h after the last DMH administration (week 7) for alkaline single-cell gel electrophoresis assay.[26] Blood samples were mixed with low-melting point agarose (100 µL 0.75% in PBS, Invitrogen), spread on slides pre-coated with normal point agarose (1.5% in PBS, Invitrogen), and coverslipped. Following agarose solidification (4°C for 5 min), coverslips were carefully removed, and slides were incubated with cold lysis solution (2.5 M NaCl, 100 mM Na_2EDTA, 10 mM Tris–HCl, 1% Triton X-100 and 10% DMSO, pH 10) overnight, at 4°C. Subsequently, the slides were immersed in fresh cold alkaline electrophoresis buffer (300 mM NaOH, 1 mM Na_2EDTA, pH > 13) for 20 min. Electrophoresis was conducted for 20 min at 1 V/cm (300 mA). The slides were neutralized with 0.4 M Tris (pH 7.5), dehydrated in 100% ethanol, and stained with SYBR Gold solution (1:10,000) (Invitrogen). Fifty randomly selected nucleoids were counted per slide (duplicate) in an epi-fluorescence microscope (Olympus BX-50) using Comet Assay IV software (Perceptive Instruments). Tail intensity (% of DNA in comet tail) was calculated.

2.3 | ACF screening

Flat-fixed colon specimens were stained with 1% methylene blue solution and topographically evaluated for ACF occurrence, considering that these lesions feature larger, darker, thicker, and "slit-like" crypts.[25] Then, the ACF number/cm^2 (mean number of ACF per colon length), aberrant crypt (AC)/cm^2 (mean number of AC per colon length), and ACF multiplicity (mean number of AC per ACF) were calculated for each group.[25]

2.4 | Immunohistochemistry

Distal colon sections (5 µm) were subjected to antigen retrieval in 0.01 M citrate buffer (pH 6.0, 5 min., 120°C) in a Pascal Pressure Chamber (Dako Cytomation). Following endogenous peroxidase blockade with 10% H_2O_2 in phosphate-buffered saline (PBS) (15 min), the slides were treated with skimmed milk (60 min) and incubated with primary antibodies directed against Ki-67 (i.e., cell proliferation, MA5-14520, 1:100 dilution, Thermo Fisher), cleaved caspase-3 (i.e., apoptosis, PA577887, 1:50 dilution, Thermo Fisher, EUA), phosphorylated-H2AX (i.e., DNA damage marker, MA5-27753, 1:200, Thermo Scientific) or β-catenin (ab32572, E247, 1:400 dilution, Abcam) in a humidified chamber (overnight, 4°C). Slides were incubated with a one-step horseradish peroxidase polymer (EasyPath - Erviegas) (20 min). The reaction was visualized

with 3-diaminobenzidine (DAB) chromogen (Sigma Aldrich), and counterstained with Harris' haematoxylin. Semiquantitative analysis for Ki-67, cleaved caspase-3, and H2AX were calculated in 15 randomly selected crypts/animal/section (distal colon). Both positive and negative epithelial cells were counted, and results were expressed as the percentage (%) of Ki-67+, cleaved caspase-3+, or H2AX+ positive cells per crypt. The analyses were performed by using Image J software (National Institutes of Health).

2.5 | Biochemical analysis

Total proteins were extracted from 50 to 100 mg of distal colon samples in KCl buffer (1.15%) and were quantified by Bradford's method. Total proteins were used to determine malondialdehyde (MDA) levels,[27] and activities of superoxide dismutase (SOD)[28] and catalase.[29] For MDA, the proteins were precipitated in a 10% trichloroacetic acid solution, centrifuged (3000 × *g*, for 5 min) and the supernatant will be removed. Thiobarbituric acid (TBA) was added in a proportion of 0.67% (1:1) and the samples were heated to 100°C (15 min). MDA reacted with TBA in a 1:2 ratio (MDA:TBA). SOD activity was measured based on the inhibition of superoxide radical reaction with pyrogallol. The catalase activity was determined in a 30% H_2O_2 PBS solution. Absorbance was measured at 535 (MDA), 420 (SOD) or 240 (catalase) nm in a microplate reader (Spectra Max 190, Molecular Devices).

2.6 | Statistical analysis

All the aforementioned analyses were performed blind. Pairwise comparisons were evaluated by the Student's *t*-test. Other data were analysed using one-way analysis of variance (ANOVA) or Kruskal-Wallis and a posteriori Tukey test. Data presentation and the number of replicates are detailed in the footnotes and captions. The aforementioned analyses were performed on Prism GraphPad software (V4.03, GraphPad Software). The level of significance was set at $p < .05$.

3 | RESULTS

3.1 | General findings

At week 7, groups showed no significant differences in initial and final body weights, absolute and relative liver weights (Table 1). At week 37, Panx1$^{-/-}$ animals exposed to DMH had decreased final body weight compared to WT counterparts ($p = .0021$). DMH-treated Panx1$^{-/-}$ mice also displayed diminished absolute and relative liver weights compared to all groups ($p < .0001$, for both) (Table 1). Colon length remained unaltered within the groups at both timepoints. Saline-treated Panx1$^{-/-}$ animals showed no alterations compared to WT counterparts. Animals presented similar diet intake in both timepoints analysed (data not shown).

TABLE 1 Implications of Pannexin 1 knockout on body weight, liver weight, and colon length during 1,2-dimethylhydrazine-induced colon carcinogenesis.

	Saline		DMH		
Parameters/Groups	**WT**	**Panx1$^{-/-}$**	**WT**	**Panx1$^{-/-}$**	***p* value**
Weeks 0–7					
n	6	6	6	6	
Initial body weight (g)	18.10 ± 1.26	17.80 ± 0.61	17.85 ± 0.51	17.55 ± 0.95	.76
Final body weight (g)	19.48 ± 0.63	19.17 ± 0.86	20.83 ± 1.03	20.33 ± 0.78	.51
Absolute liver weight (g)	0.97 ± 0.10	1.05 ± 0.08	0.92 ± 0.11	1.05 ± 0.09	.07
Relative liver weight (%)	4.36 ± 0.30	4.90 ± 0.27	4.75 ± 0.23	5.18 ± 0.49	.055
Colon length (cm)	10.00 ± 0.56	9.66 ± 0.51	10.31 ± 0.76	9.17 ± 1.25	.13
Weeks 0–37					
n	12	12	12	12	
Initial body weight (g)	17.30 ± 0.92	17.33 ± 1.22	18.26 ± 0.69	17.96 ± 1.72	.15
Final body weight (g)	24.16 ± 2.65 ab	25.65 ± 2.09 a	23.50 ± 2.53 ab	22.03 ± 1.03 b	.0021
Absolute liver weight (g)	1.07 ± 0.19 a	1.07 ± 0.14 a	0.95 ± 0.14 a	0.73 ± 0.15 b	<.0001
Relative liver weight (%)	4.68 ± 0.60 a	4.20 ± 0.39 ab	4.03 ± 0.38 b	3.32 ± 0.68 c	<.0001
Colon length (cm)	9.95 ± 1.05	9.50 ± 0.95	9.93 ± 0.97	9.59 ± 0.63	.51

Note: WT: wild-type. *n* = number of mice/group/genotype. Data are presented as mean + standard deviation. Different letters correspond to statistical difference among groups by one-way ANOVA and a posteriori Tukey test ($p < .05$). The *p* value in the tables refers to the ANOVA-derived analysis.

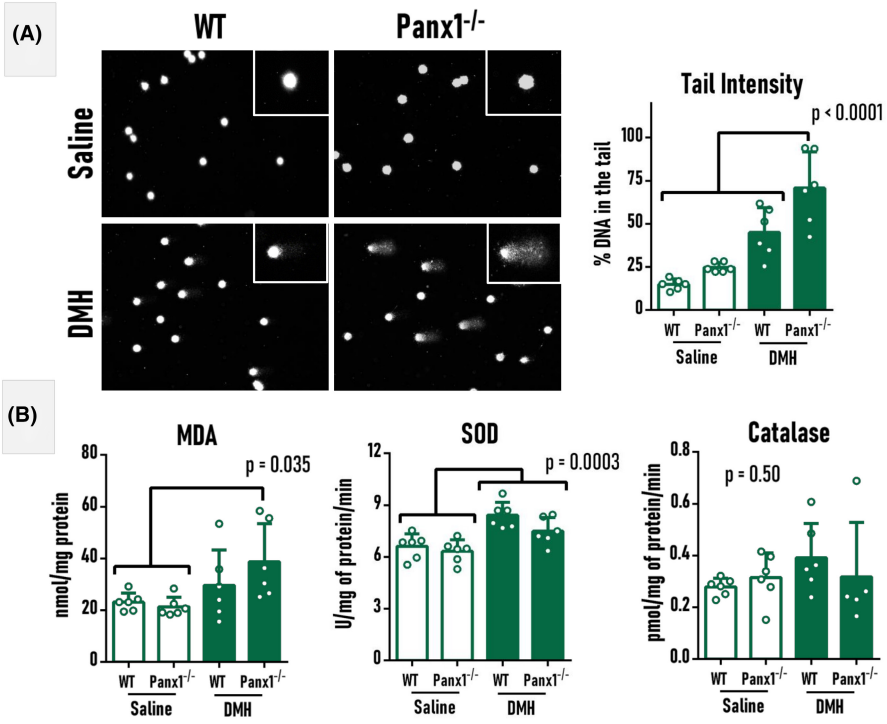

FIGURE 2 Effects of pannexin 1 knockout (Panx1$^{-/-}$) on (A) peripheral blood genotoxicity, (B) malondialdehyde (MDA) levels and antioxidant superoxide dismutase (SOD) and catalase activities in the colon during 1,2-dimethylhydrazine (DMH)-induced colon carcinogenesis in mice at week 7. WT: wild-type. $n = 6$ mice/group/genotype. Data are presented as mean + standard deviation, and data points. Data were analysed by one-way ANOVA and a posteriori Tukey test ($p < .05$). The p value in the graphs refers to the ANOVA-derived analysis.

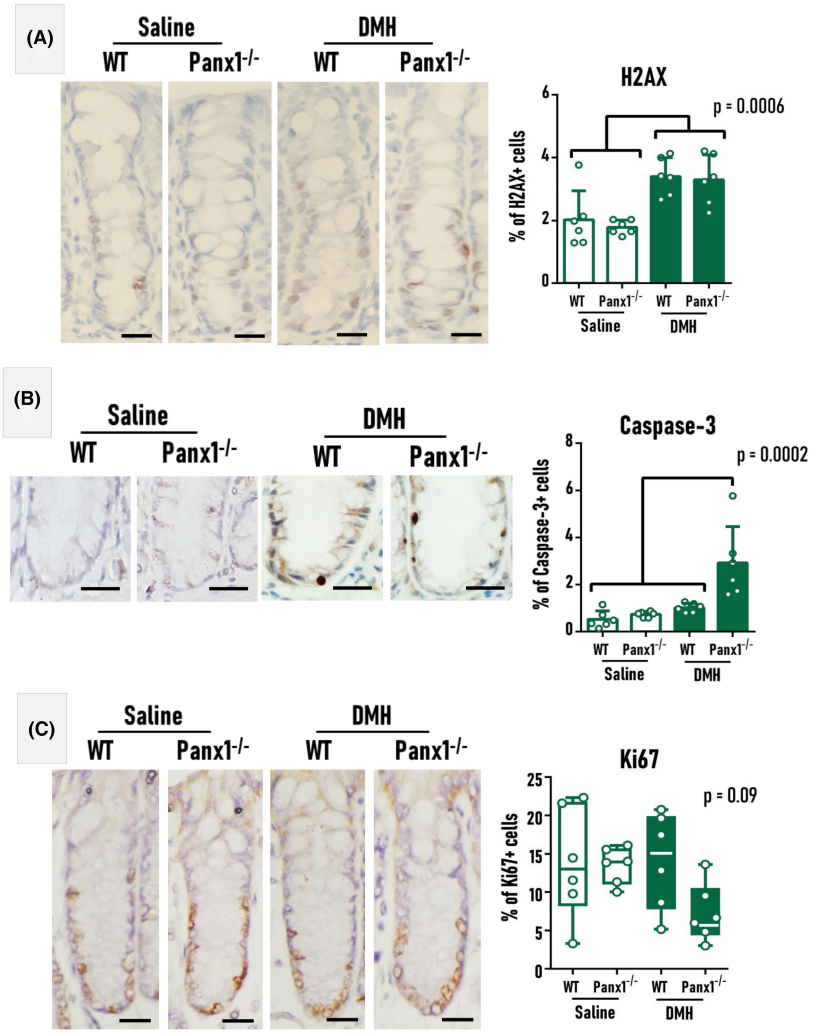

FIGURE 3 Effects of pannexin 1 knockout (Panx1$^{-/-}$) on (A) colonocyte genotoxicity (H2AX), (B) crypt apoptosis (caspase-3), and (C) proliferation (Ki67) and during 1,2-dimethylhydrazine (DMH)-induced colon carcinogenesis in mice at week 7. Representative microscopic overviews (scale bar: 10 μm) show that H2AX and Ki67 labelling comprised top, middle and/or bottom crypt compartments, while caspase-3 was restricted to bottom crypt compartment. WT: wild-type. $n = 6$ mice/group/genotype. Data are presented as mean + standard deviation or box plots, and data points. Data were analysed by one-way ANOVA (H2AX and caspase-3) or Kruskal–Wallis (Ki-67) and a posteriori Tukey test ($p < .05$). The p value in the graphs refers to the ANOVA-derived analysis.

3.2 | Panx1 knockout promotes carcinogen-induced peripheral blood genotoxicity and lipid peroxidation in the colon at week 7

Four hours after the last carcinogen administration, we observed that Panx1 ablation increased the DMH-induced genotoxicity in nucleated peripheral blood cells, as inferred by comet assay ($p < .0001$) (Figure 2A). Eight hours after the last carcinogen administration, although we found that Panx1 deletion resulted in no alterations in the DMH-mediated increase in the number of colonocytes positive for H2AX (Figure 3A) - an indicator of double-strand DNA breaks[30] – Panx1 knockout did result in higher DMH-induced MDA levels in the colon ($p = .035$) (Figure 2B), which is an oxidative stress byproduct involved implicated in adduct formation, cytotoxicity and cell death.[31] These findings are in line with the increase in cleaved caspase-3 immunolabelling index in the colonic crypts of DMH-exposure Panx1$^{-/-}$ mice ($p = .0002$) (Figure 3B). The activities of SOD, and catalase (Figure 2B), and the proliferation of colonocytes (Ki67) (Figure 3C) remained unaltered by Panx1 genetic ablation.

3.3 | Panx1 knockout increases preneoplastic ACF burden at week 37

Thirty weeks after the last carcinogen administration, Panx1$^{-/-}$ animals showed increased ACF ($p = .0039$), AC ($p = .026$) and ACF multiplicity ($p = .005$) by 56%, 57% and 20%, respectively, compared to the WT counterpart (Figure 4). Representative microscopic overview of these lesions in haematoxylin and eosin (HE)-stained sections are also shown (Figure 5).

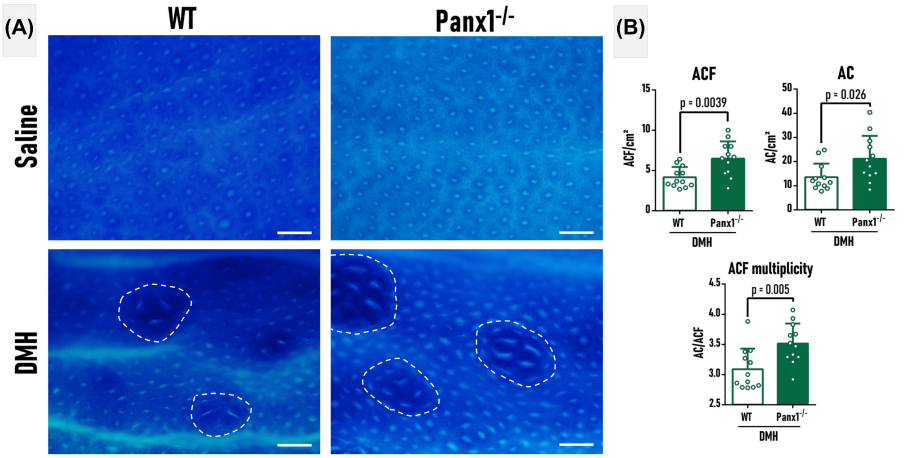

FIGURE 4 Effects of pannexin 1 knockout (Panx1$^{-/-}$) on aberrant crypt foci (ACF) burden during 1,2-dimethylhydrazine (DMH)-induced colon carcinogenesis in mice at week 37. (A) Representative photomicrographs of a whole mount of colon specimens stained with methylene blue (scale bar: 100 μm) – depicting the absence (non-initiated) or the occurrence of ACF (DMH-initiated mouse) (dotted lines). (B) Colon length, ACF, aberrant crypt (AC), and ACF multiplicity (AC/ACF) data in both genotypes. $n = 12$ mice/group/genotype. WT: wild type. Data are presented as mean + standard deviation, and data points. Data were analysed by Student's *t*-test ($p < .05$). The *p* value in the graphs refers to the ANOVA-derived analysis.

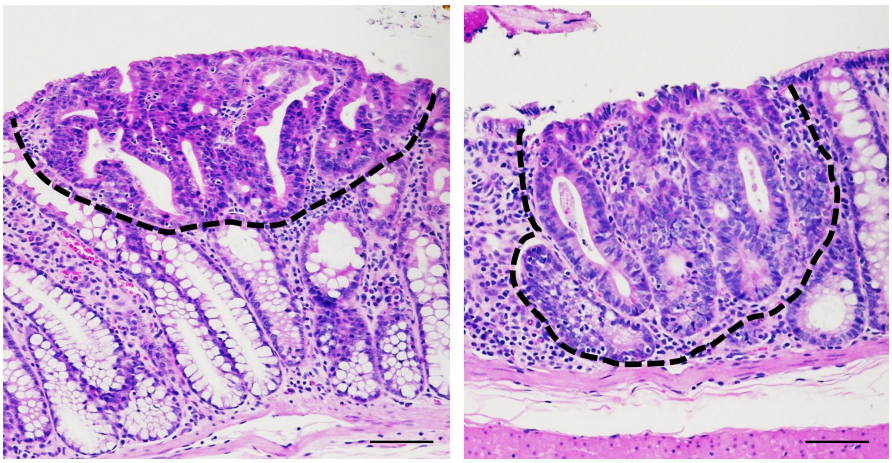

FIGURE 5 Representative photomicrographs of dimethylhydrazine (DMH)-induced aberrant crypt foci (ACF) – featuring dysplastic phenotype – in haematoxylin and eosin (HE)-stained sections (dotted lines, scale bar: 50 μm).

4 | DISCUSSION

In the present investigation, we examined the modifying effects of Panx1 global ablation on the early events involved in chemically induced colon carcinogenesis in mouse, evaluating both (A) the sub-acute toxicity outcomes and (B) preneoplastic lesion burden. In brief, regarding the sub-acute effects, the genetic removal of Panx1 resulted in heightened genotoxicity induced by DMH in peripheral blood cells. It also led to elevated levels of MDA in the colon and increased apoptosis (cleaved caspase-3) in colonic crypts. Importantly, at the later timepoint, animals lacking Panx1 exhibited a decreased body weight and showed a 56% increase in mean number of aberrant ACF and a 20% increase in ACF multiplicity. Of note, the Panx1 KO did not exert any noticeable impact on all the measured parameters in mice treated with saline. Overall, our findings suggest that the genetic elimination of Panx1 fosters the formation of preneoplastic aberrant crypt foci (ACF) during chemically induced colon carcinogenesis in mice. Conversely, our observations propose a protective role of Panx1 in the early steps of this process. The genetically ablated Panx1 mice were used since these animals are functional knockouts that express a truncated form of active Panx1 subunits.[21] This model is considered a useful tool for biomedical research, including the investigation of Panx1 roles on gastrointestinal diseases.[32–34]

DMH is an alkylating colon-specific complete procarcinogen. DMH is first metabolically activated by hepatic cytochrome P450 (CYP) enzymes, primarily CYP2E1 and CYP2A6, through N-demethylation. This, methyl diazonium, methyl ions and other reactive species are generated, reaching the colon via the bloodstream.[8] In the colon, DMH metabolites alkylate colonocytes, "initiating" them for colon carcinogenesis.[8,23] Furthermore, other secondary reactive metabolites may also be generated as DMH-derived radicals that react with membrane lipids, as MDA, which is a known marker of oxidative stress/lipid peroxidation.[9,31] MDA is formed through the process of lipid peroxidation. Lipid peroxidation occurs when reactive oxygen species (ROS), such as free radicals, attack and react with polyunsaturated fatty acids (PUFAs) present in cell membranes.[31] When evaluating the sub-acute toxicity outcomes at week 7, we observed that Panx1 deletion promoted the carcinogen-induced systemic genotoxicity, also increasing MDA levels in whole colon samples and the number of caspase-3 positive colonic epithelial cells. MDA is a highly reactive and cytotoxic molecule. It can form adducts with proteins, DNA, and other biomolecules, leading to cellular damage, dysfunction and death. Thus, at early this timepoint, the increased apoptosis in epithelial colonic cells observed in Panx1 deletion is probably a response to the increased MDA levels. It is also important to point out that the increase in lipid peroxidation is clearly implicated on CC pathogenesis in humans and in preclinical models.[35,36] Panx1 hemichannels and oxidative stress have an intimate bidirectional relationship. Reactive species may negatively regulate Panx1 hemichannel activity, as nitric oxide (NO)-induced structural modification of Panx1 protein resulted in the inhibition of the hemichannel in human embryonic kidney cells.[37] On the other hand, the Panx1-mediated release of ATP activated P2Y/P2X receptors, subsequent G proteins, triggering the accumulation of NADPH oxidases-generated reactive species in vitro.[38] Although our findings may sound contrasting, most of the available findings mechanistically linking Panx1 and oxidative stress are restricted to in vitro bioassays in physiological contexts. Thus, further molecular investigations on Panx1 KO in the multistage colon carcinogenesis context are necessary.

At week 37, we observed that animals lacking Panx1 had decreased body and liver weights, and increased preneoplastic ACF burden. As diminished body and liver weights are known effects of DMH upon multiple administrations,[39,40] the findings indicate that Panx1 knockout may predispose mice to these deleterious toxicological outcomes. As ACF are the earliest morphological manifestation of colon carcinogenesis, the modulation of these classical parameters is predictive of the preventive or predisposing interventions. In both preclinical and clinical investigations, the occurrence of ACF positively correlates with colon tumorigenesis.[6,7] Thus, the findings indicate that Panx1 knockout may promote the early stages of DMH-induced colon carcinogenesis. The promotion of lipid peroxidation by $Panx1^{-/-}$ at week 7 is proposed to be partly involved to the enhanced ACF burden at week 37, although other predisposing mechanisms should be considered regardless of carcinogen-related ones. In general, recent findings from human tumours and several tumour-derived cell lines indicate that high Panx1 expression enables survival advantages to tumours, increasing their potential for progression.[16–19,41] Nonetheless, the attenuation of Panx1 does not have a common outcome in all cancers. In human oral cancer cells, the microRNA-mediated Panx1 downregulation is proposed as a chemotherapy resistance mechanism, as the inhibition of Panx1 hemichannels may negatively interfere with ATP discharge that contributes to chemotherapy-induced tumour cell apoptosis.[42] Panx1 is expressed in immune cells that infiltrate tumours and promote antitumor immunity.[43] In a certain way our findings are in line with Derangère et al.,[20] in the sense that Panx1 may have a tumour suppressor role of Panx1 in CC cells, although this study addresses

the progression (malignant) stage of colon carcinogenesis and not the preneoplastic step. Differently from these findings, on which Panx1 was associated with a pyroptosis mechanism by the activation of LXRβ/Panx1/NLRP3/caspase-1-pathway in CC cells, our increased caspase-3 labelling may be a response to the enhanced oxidative stress right after carcinogen exposure. It is noteworthy that preneoplastic stages – as ACF - are usually underappreciated in the available bioassays. As Panx1 (and hemichannels) may have a complex interplay with a myriad of cellular and non-cellular components of tumour microenvironment, the preventive, suppressive or promoting outcomes should consider late stage of disease, and others tumour types. Considering that saline-treated Panx1 ablated mice did not developed ACF, and did not spontaneously develop tumours in previous assays,[41] the suppressive role of this protein in carcinogenesis should not be overestimated as well.

In essence, our findings innovatively indicate that Panx1 genetic ablation promotes preneoplastic ACF development during early stage of chemically-induced mouse colon carcinogenesis. A protective role of Panx1 on colon carcinogenesis is postulated, although further investigation is required in late stages of this disease.

ACKNOWLEDGEMENT

Authors thank Dr. Valery I. Shestopalov (Bascom Palmer Eye Institute, Department of Ophthalmology, University of Miami Miller School of Medicine, 1638 NW 10th Avenue, 33136 Miami, Florida, United States), that kindly donated Panx1$^{-/-}$ mice.

FUNDING INFORMATION

Bruno Cogliati was the recipient of support research from the São Paulo Research Foundation (FAPESP, grant #2018/10953–9, and #2022/02175–1). Guilherme R. Romualdo was the recipient of scholarship and grants from FAPESP (2022/06082-8 and 2023/08751-7). Sara Gomes Espírito Santo was the recipient of a regular scholarship (88887.600918/2021-00), and an international exchange program fellowship (88887.716728/2022-00) from Coordenação de Aperfeiçoamento de Pessoal de Nível Superior -Brasil (CAPES-PrInt). This study was financed in part by CAPES - Finance Code 001. The funders did not influence the writing and interpretation of data.

CONFLICT OF INTEREST STATEMENT

The authors declare no conflict of interest.

ORCID

Guilherme Ribeiro Romualdo https://orcid.org/0000-0001-5320-8380

REFERENCES

1. Sung H, Ferlay J, Siegel RL, et al. Global cancer statistics 2020: GLOBOCAN estimates of incidence and mortality worldwide for 36 cancers in 185 countries. *CA Cancer J Clin*. 2021;71:209-249. doi:10.3322/caac.21660
2. Vieira AR, Abar L, Chan DSM, et al. Foods and beverages and colorectal cancer risk: a systematic review and meta-analysis of cohort studies, an update of the evidence of the WCRF-AICR continuous update project. *Ann Oncol*. 2017;28:1788-1802. doi:10.1093/annonc/mdx171
3. Sawicki T, Ruszkowska M, Danielewicz A, Niedźwiedzka E, Arłukowicz T, Przybyłowicz KE. A review of colorectal cancer in terms of epidemiology, risk factors, development, symptoms and diagnosis. *Cancer*. 2021;13:1-23. doi:10.3390/cancers13092025
4. Amitay EL, Carr PR, Jansen L, et al. Smoking, alcohol consumption and colorectal cancer risk by molecular pathological subtypes and pathways. *Br J Cancer*. 2020;122:1604-1610. doi:10.1038/s41416-020-0803-0
5. Wang J, Li S, Liu Y, Zhang C, Li H, Lai B. Metastatic patterns and survival outcomes in patients with stage IV colon cancer: a population-based analysis. *Cancer Med*. 2020;9:361-373. doi:10.1002/cam4.2673
6. Wargovich MJ, Brown VR, Morris J. Aberrant crypt foci: the case for inclusion as a biomarker for colon cancer. *Cancer*. 2010;2:1705-1716. doi:10.3390/cancers2031705
7. Clapper ML, Chang WCL, Cooper HS. Dysplastic aberrant crypt foci: biomarkers of early colorectal neoplasia and response to preventive intervention. *Cancer Prev Res*. 2020;13:229-239. doi:10.1158/1940-6207.CAPR-19-0316
8. Perše M, Cerar A. Morphological and molecular alterations in 1,2 dimethylhydrazine and azoxymethane induced colon carcinogenesis in rats. *J Biomed Biotechnol*. 2011;2011:473964. doi:10.1155/2011/473964
9. Caetano BFR, Tablas MB, Romualdo GR, et al. Early molecular events associated with liver and colon sub-acute responses to 1,2-dimethylhydrazine: potential implications on preneoplastic and neoplastic lesion development. *Toxicol Lett*. 2020;329:67-79. doi:10.1016/j.toxlet.2020.04.009
10. Amadeu SO, Sarmiento-Machado LM, Bartolomeu AR, et al. *Arthrospira* (spirulina) *platensis* feeding reduces the early stage of chemically induced rat colon carcinogenesis. *Br J Nutr*. 2020;129:1-11. doi:10.1017/s0007114522001350
11. Bartolomeu AR, Romualdo GR, Lisón CG, et al. Caffeine and chlorogenic acid combination attenuate early-stage chemically induced colon carcinogenesis in mice: involvement of oncomiR miR-21a-5p. *Int J Mol Sci*. 2022;23:6292. doi:10.3390/ijms23116292
12. Bond SR, Naus CC. The pannexins: past and present. *Front Physiol*. 2014;5:58. FEB:1–24. doi:10.3389/fphys.2014.00058
13. Chiu YH, Ravichandran KS, Bayliss DA. Intrinsic properties and regulation of pannexin 1 channel. *Channels*. 2014;8:103-109. doi:10.4161/chan.27545
14. Maes M, Crespo Yanguas S, Willebrords J, Cogliati B, Vinken M. Connexin and pannexin signaling in gastrointestinal and liver disease. *Transl Res*. 2015;166:332-343. doi:10.1016/j.trsl.2015.05.005
15. Diezmos EF, Sandow SL, Markus I, et al. Expression and localization of pannexin-1 hemichannels in human colon in health and disease. *Neurogastroenterol Motil*. 2013;25:e395-e405. doi:10.1111/nmo.12130

16. Ying W, Zheng K, Wu Y, Wang O. Pannexin 1 mediates gastric cancer cell epithelial–mesenchymal transition via aquaporin 5. *Biol Pharm Bull*. 2021;44:1111-1119. doi:10.1248/bpb.b21-00292
17. Jalaleddine N, El-Hajjar L, Dakik H, et al. Pannexin1 is associated with enhanced epithelial-to-mesenchymal transition in human patient breast cancer tissues and in breast cancer cell lines. *Cancer*. 2019;11:1-22. doi:10.3390/cancers11121967
18. Shi G, Liu C, Yang Y, et al. Panx1 promotes invasion-metastasis cascade in hepatocellular carcinoma. *J Cancer*. 2019;10:5681-5688. doi:10.7150/jca.32986
19. Bao L, Sun K, Zhang X. PANX1 is a potential prognostic biomarker associated with immune infiltration in pancreatic adenocarcinoma: a pan-cancer analysis. *Channels*. 2021;15:680-696. doi:10.1080/19336950.2021.2004758
20. Derangère V, Chevriaux A, Courtaut F, et al. Liver X receptor β activation induces pyroptosis of human and murine colon cancer cells. *Cell Death Differ*. 2014;21:1914-1924. doi:10.1038/cdd.2014.117
21. Dvoriantchikova G, Ivanov D, Barakat D, et al. Genetic ablation of Pannexin1 protects retinal neurons from ischemic injury. *PloS One*. 2012;7:1-10. doi:10.1371/journal.pone.0031991
22. Richards TC. Early changes in the dynamics of crypt cell populations in mouse colon following administration of 1,2-dimethylhydrazine. *Cancer Res*. 1977;37:1680-1685.
23. James JT, Shamsuddin AM, Trump BF. Comparative study of the morphologic, histochemical, and proliferative changes induced in the large intestine of ICR/ha and C57BL/ha mice by 1,2-dimethylhydrazine. *J Natl Cancer Inst*. 1983;71:955-964.
24. Ijiri K. Apoptosis (cell death) induced in mouse bowel by 1,2-dimethylhydrazine, methylazoxymethanol acetate, and gamma-rays. *Cancer Res*. 1989;49:6342-6346.
25. Bird RP. Observation and quantification of aberrant crypts in the murine colon treated with a colon carcinogen: preliminary findings. *Cancer Lett*. 1987;37:147-151.
26. Sasaki YF, Saga A, Akasaka M, et al. Organ-specific genotoxicity of the potent rodent colon carcinogen 1,2-dimethylhydrazine and three hydrazine derivatives: difference between intraperitoneal and oral administration. *Mutat Res*. 1998;415:1-12.
27. Buege JA, Aust SD. Microsomal lipid peroxidation methods. *Enzymol*. 1987;52:302-310. doi:10.1016/s0076-6879(78)52032-6
28. Marklund S, Marklund G. Involvement of the superoxide anion radical in the autoxidation of pyrogallol and a convenient assay for superoxide dismutase. *Eur J Biochem*. 1974;47:469-474. doi:10.1111/j.1432-1033.1974.tb03714.x
29. Bergmeyer HU. *Methods of Enzymatic Analysis*. 2nd ed. Academic Press; 1974.
30. Mah LJ, El-Osta A. Karagiannis TC.γh2AX: a sensitive molecular marker of DNA damage and repair. *Leukemia*. 2010;24:679-686.
31. Ayala A, Muñoz MF, Argüelles S. Lipid peroxidation: production, metabolism, and signaling mechanisms of malondialdehyde and 4-hydroxy-2-nonenal. *Oxid Med Cell Longev*. 2014;2014:360438. doi:10.1155/2014/360438
32. Crespo Yanguas S, da Silva TC, Pereira IVA, et al. Genetic ablation of pannexin1 counteracts liver fibrosis in a chemical, but not in a surgical mouse model. *Arch Toxicol*. 2018;92:2607-2627. doi:10.1007/s00204-018-2255-3
33. Hanstein R, Negoro H, Patel NK, et al. Promises and pitfalls of a Pannexin1 transgenic mouse line. *Front Pharmacol*. 2013;4:61. MAY:1–10. doi:10.3389/fphar.2013.00061
34. Willebrords J, Maes M, Pereira IVA, et al. Protective effect of genetic deletion of pannexin1 in experimental mouse models of acute and chronic liver disease. *Biochim Biophys Acta - Mol Basis Dis*. 2018;1864:819-830. doi:10.1016/j.bbadis.2017.12.013
35. Skrzydlewska E, Sulkowski S, Koda M, Zalewski B, Kanczuga-Koda L, Sulkowska M. Lipid peroxidation and antioxidant status in colorectal cancer. *World J Gastroenterol*. 2005;11:403-406. doi:10.3748/wjg.v11.i3.403
36. Lei L, Zhang J, Decker EA, Zhang G. Roles of lipid peroxidation-derived electrophiles in pathogenesis of colonic inflammation and colon cancer. Front cell. *Dev Biol*. 2021 May;17(9):665591. doi:10.3389/fcell.2021.665591
37. Poornima V, Vallabhaneni S, Mukhopadhyay M, Bera AK. Nitric oxide inhibits the pannexin 1 channel through a cGMP-PKG dependent pathway. *Nitric Oxide - Biol Chem*. 2015;47:77-84. doi:10.1016/j.niox.2015.04.005
38. Hung SC, Choi CH, Said-Sadier N, et al. P2X4 assembles with P2X7 and Pannexin-1 in gingival epithelial cells and modulates ATP-induced reactive oxygen species production and inflammasome activation. *PloS One*. 2013;8:e70210. doi:10.1371/journal.pone.0070210
39. Ali MS, Hussein RM, Gaber Y, Hammam OA, Kandeil MA. Modulation of JNK-1/ β-catenin signaling by: *Lactobacillus casei*, inulin and their combination in 1,2-dimethylhydrazine-induced colon cancer in mice. *RSC Adv*. 2019;9:29368-29383. doi:10.1039/c9ra04388h
40. Hori H, Shimoyoshi S, Tanaka Y, et al. Multiple-endpoint genotoxicity assay for colon carcinogen 1,2-dimethylhydrazine. *Mutat Res - Genet Toxicol Environ Mutagen*. 2020;849:503130. doi:10.1016/j.mrgentox.2019.503130
41. Laird DW, Penuela S. Pannexin biology and emerging linkages to cancer. *Trends Can*. 2021;7:1119-1131. doi:10.1016/j.trecan.2021.07.002
42. Yokoyama S, Shigeishi H, Murodumi H, et al. Effects of miR-224-5p-enhanced downregulation of pannexin-1 on docetaxel-induced apoptosis in amoeboid-like CD44high oral cancer cells. *Eur J Oral*. 2021;129:e12812. doi:10.1016/10.1111/eos.12812
43. Woehrle T, Yip L, Manohar M, et al. Hypertonic stress regulates T cell function via pannexin-1 hemichannels and P2X receptors. *J Leukoc Biol*. 2010;88:1181-1189. doi:10.1189/jlb.0410211

How to cite this article: Espírito Santo SG, Da Silva TC, Cogliati B, Barbisan LF, Romualdo GR. Panx1 knockout promotes preneoplastic aberrant crypt foci development in a chemically induced model of mouse colon carcinogenesis. *Int J Exp Path*. 2023;104:304-312. doi:10.1111/iep.12491